

ODDR: Outlier Detection & Dimension Reduction Based Defense Against Adversarial Patches

Nandish Chattopadhyay*¹, Amira Guesmi*¹, Muhammad Abdullah Hanif¹
Bassem Ouni², Muhammad Shafique¹

¹ eBrain Lab, Division of Engineering, New York University (NYU) Abu Dhabi, UAE

² AI and Digital Science Research Center, Technology Innovation Institute (TII), Abu Dhabi, UAE

Abstract

Adversarial attacks are a major deterrent towards the reliable use of machine learning models. A powerful type of adversarial attacks is the patch-based attack, wherein the adversarial perturbations modify localized patches or specific areas within the images to deceive the trained machine learning model. In this paper, we introduce Outlier Detection and Dimension Reduction (ODDR), a holistic defense mechanism designed to effectively mitigate patch-based adversarial attacks. In our approach, we posit that input features corresponding to adversarial patches, whether naturalistic or otherwise, deviate from the inherent distribution of the remaining image sample and can be identified as outliers or anomalies. ODDR employs a three-stage pipeline: Fragmentation, Segregation, and Neutralization, providing a model-agnostic solution applicable to both image classification and object detection tasks. The Fragmentation stage parses the samples into chunks for the subsequent Segregation process. Here, outlier detection techniques identify and segregate the anomalous features associated with adversarial perturbations. The Neutralization stage utilizes dimension reduction methods on the outliers to mitigate the impact of adversarial perturbations without sacrificing pertinent information necessary for the machine learning task. Extensive testing on benchmark datasets and state-of-the-art adversarial patches demonstrates the effectiveness of ODDR. Results indicate robust accuracies matching and lying within a small range of clean accuracies (1% – 3% for classification and 3% – 5% for object detection), with only a marginal compromise of 1% – 2% in performance on clean samples, thereby significantly outperforming other defenses.

1. Introduction

Adversarial attacks pose a formidable threat to the robustness and performance of highly trained deep neural network (DNN) models [2, 11, 18]. In these attacks, an adversary strategically introduces adversarial perturbations to test samples, causing significant disruptions to the model’s accurate predictions. A particularly potent manifestation of adversarial attacks involves the insertion of localized patches into test images. By exploiting this vulnerability, attackers force the DNN model to make errors in critical tasks such as image classification or object detection [12, 13, 16].

Patch-based attacks stand out as a widely recognized and practical form of adversarial attacks due to their adaptability, particularly in situations with limited access [13]. In contrast to conventional adversarial techniques that require extensive perturbations across the entire target object, patch-based attacks showcase a localized nature. These attacks operate like discreet stickers, allowing them to be effortlessly applied to potential targets—simulating real-world scenarios where adversaries may encounter constraints in resources or access. The subtle characteristics of patch-based attacks contribute to their elusive nature, emphasizing the urgent need for the swift implementation of robust defense mechanisms.

Defense mechanisms against such attacks aim to locate and neutralize the adversarial patches [5, 17, 21, 24, 26]. However, these defenses are susceptible to generating false positives [21] and exhibit difficulty in accurately distinguishing between adversarial examples and clean samples. Additionally, in some cases, these defenses might remove or alter important features [17, 26], causing the model’s performance to degrade even on benign samples.

We posit that these patches manifest as outliers or anomalies within the distribution of incoming images. The adversarial noise contained in the patches is out-of-distribution as compared to the signal/information in the rest of the sample. Employing cutting-edge anomaly

*These authors contributed equally to this work

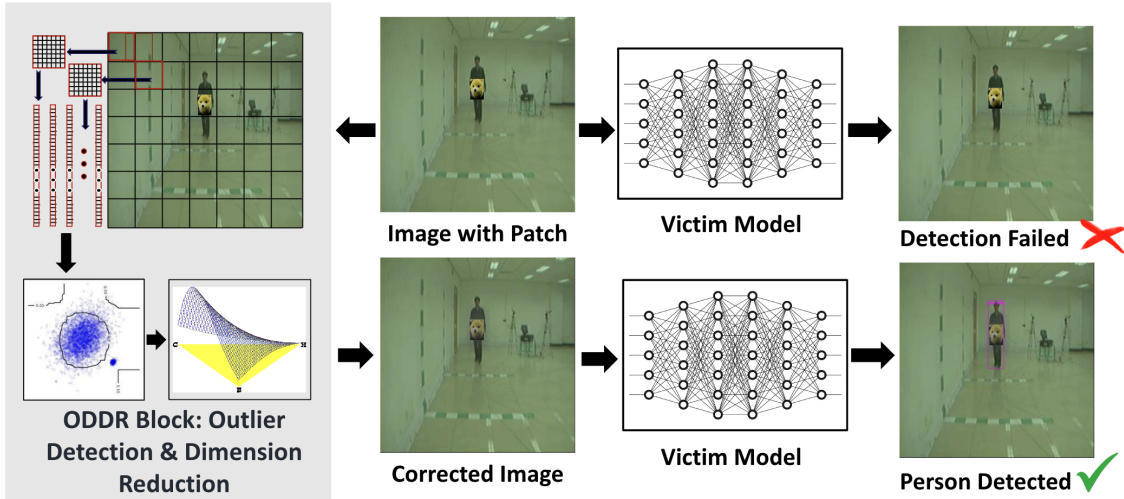


Figure 1. ODDR: Outlier Detection and Dimension Reduction to thwart adversarial patch based attack.

detection techniques allows for the segregation of these patches if they deviate from the overall image distribution. Experimental results affirm the validity of this approach, demonstrating the effective detection of patches as outliers. We report the success of using properly tuned adaptations of standard outlier detection techniques in identifying the adversarial noise within the patches.

For the second aspect of the problem, having identified the region that contains the adversarial patch, rather than relying on intricate and computationally intensive neural network-based patch neutralization techniques, we advocate for the use of simple Dimensionality Reduction. Through matrix-based transformations, this approach proves adept at nullifying the impact of the patch without wholesale destruction of surrounding pertinent information. This information is often critical for the underlying machine learning task. Our experimental findings, illustrated in Figure 1, substantiate the efficacy of our proposed approach.

Novel Contributions – The main contributions of this paper are summarized as follows:

- We propose a method that identifies and locates adversarial patches by detecting clusters of outliers within the input features derived from the image. Employing strategic dimension reduction on a window over the detected cluster of outliers, our approach effectively neutralizes the adversarial patch while preserving valuable information in its vicinity.
- We present a robust Outlier Detection and Dimension Reduction (ODDR) technique. This technique is developed as a streamlined 3-stage pipeline: Fragmentation, Segregation, and Neutralization. ODDR serves as a versatile and easily implementable adversarial defense mechanism.

- We demonstrate the efficacy and versatility of the proposed ODDR technique as a model-agnostic defense against adversarial patches. This defense is applicable to both image classification and object detection tasks. In fact, our defense achieves 79.1% robust accuracy when countering GoogleAP [9] attack on the ImageNet [7] dataset with 2% loss in baseline accuracy.
- Similarly, for detection tasks, our defense achieves 93.54% and 83.21% robust average precision when countering AdvYOLO attack [25] on the CASIA [27] and INRIA [6] datasets, respectively.
- Our proposed technique ensures resilience against realistic and naturalistic adversarial patches. This addresses the challenges posed by more sophisticated and nuanced attack scenarios. Our defense achieves 87.5% and 65% robust average precision when defending against Naturalistic patch attack [16] on CASIA and INRIA datasets, respectively.

2. Theoretical Background

In this section, we delve into the foundational theoretical principles that constitute the building blocks of the proposed ODDR scheme. We expound upon the dual components of the defense mechanism.

2.1. Segregating Input Features

We use the Isolation Forest algorithm as a robust tool for detecting outliers and anomalies within datasets. Operating under the paradigm of Unsupervised Learning, this technique excels in scenarios where labeled data is unavailable, making it particularly versatile in diverse applications. Noteworthy is the algorithm’s deployment of Binary Decision Trees through a bagging approach,

drawing parallels to the well-known Random Forest technique employed in supervised learning. The core hypothesis guiding Isolation Forest is predicated on the assumption that anomalies represent a minority within the dataset, comprising fewer instances than their normal counterparts. Additionally, these anomalies are posited to possess attribute-values that diverge from those associated with normal instances. In simpler terms, anomalies are characterized as being both fewer in number and different from the rest of the samples [20]. This particularly makes it a good fit for detecting adversarial patches from input features of the test samples. Leveraging these assumptions, Isolation Forest excels in isolating anomalies by constructing an ensemble of Binary Trees for a given dataset. Anomalies, given their distinctive nature, tend to exhibit shorter paths within these trees compared to normal instances [14].

2.2. Outlier Detection

Let's formally define the mechanism of constructing an isolation tree for the purpose of detecting outliers. Consider a dataset $X = \{x_1, \dots, x_n\}$, comprising n vectors representing instances from a multivariate distribution of dimension d . To build the isolation tree, the dataset X undergoes a recursive division process based on the random selection of an attribute q and a corresponding threshold value p . This process continues until one of the following three conditions is met:

- the isolation tree attains maximum permissible height
- $|X| = 1$
- the data in the dataset X has equal values

The attainment of the objective in anomaly or outlier detection hinges on the ability to rank samples, reflecting their degree of anomaly. This ranking can be accomplished by applying a sorting algorithm to the path lengths or anomaly scores associated with each sample. Consequently, the definition of anomaly scores becomes imperative in this context.

The path length $h(x)$ for a sample point x is defined as the count of nodes that x traverses in the isolation tree from the root node to the conclusion of the traversal at an external node. Drawing on the structural similarities between isolation trees and Binary Search Trees, it can be inferred that the estimated average path length aligns with that of an unsuccessful search in a Binary Search Tree. Well-established in the literature, it is known that for a dataset comprising n samples, the average path length of an unsuccessful search is:

$$c(n) = 2H(n-1) - (2(n-1)/n), \quad (1)$$

with $H(i)$ denoting the Harmonic number, estimated as $\ln(i) + 0.57721567$ [Euler's constant]. Additionally, $c(n)$

represents the mean of $h(x)$ over n . Consequently, the anomaly score s can be defined as:

$$Score(x) = s(x, n) = 2^{-\frac{E(h(x))}{c(n)}} \quad (2)$$

where $E(h(x))$ represents the mean of $h(x)$ derived from the isolation forest, which is constructed from multiple isolation trees. It follows that when $E(h(x)) \rightarrow c(n)$, $s \rightarrow 0.5$; when $E(h(x)) \rightarrow 0$, $s \rightarrow 1$; and when $E(h(x)) \rightarrow n-1$, $s \rightarrow 0$. The interpretation of the anomaly score s is as follows:

- If the samples possess an anomaly score close to unity, they are highly likely to be outliers.
- Those with a score much smaller than 0.5 are likely to belong to the distribution.
- If a significant portion of samples returns a score around the 0.5 mark, it is highly probable that there are not many outliers in the dataset.

Isolation Forest exhibits swift convergence even with a minimal number of trees, and the incorporation of subsampling enhances its ability to yield favorable results while maintaining computational efficiency. The algorithm operates through a recursive process of generating partitions on the dataset, achieved by randomly selecting features and subsequently assigning random split values for these features. Anomalies are identified by their shorter path lengths within the tree structure, with path length denoting the number of edges traversed from the root node.

2.3. Dimension Reduction

Dimension Reduction has been successfully used as a method of mitigating adversarial attacks [3, 4]. This technique maps the input into a lower dimensional space, preserving a chosen amount of variability, thereby getting rid of significant proportion of the adversarial noise. This is a standard technique that is used in linear algebra for decomposing a matrix, like the portions of images in our use-case, into components which are able to express the informational variability of the original matrix in useful forms [10]. Intuitively, this projects the matrix on to an orthonormal basis and the variability within it is expressed as a linear combination of the components. At first, if we consider that an image (a coloured image has three channels and therefore three such matrices) is a $m \times n$ -matrix M , then one can use Singular Value Decomposition to factorize the same into $M = U\Sigma V^T$, where U and V are orthogonal matrices and $\Sigma = \text{diag}(\sigma_1, \dots, \sigma_r)$, where $r = \min(m, n)$ such that $\sigma_1 \geq \dots \geq \sigma_r \geq 0$. In this case, the singular values are the σ_i s, and thereby we have the top r columns of V and U being the right and left singular vectors respectively. This formulation is necessary for dimensionality reduction using Truncated Singular Value Decomposition as explained hereafter. For the matrix M with a rank r , one can represent $M = U_r \Sigma_r V_r^T$ where U_r

and V_r comprises of the left and right singular vectors. For any k , such that ($k < r$), one can therefore obtain M_k , where $M_k = U_k \Sigma_k V_k^T$, which is lower rank approximation of the matrix. This is used in dimensionality reduction, facilitated by the fact that the singular values are so arranged such that they provide the ordering of the information contained in such truncated approximations. Specifically, in our implementation, we have used the proportion of the singular values as a surrogate to estimate the amount of information preserved upon the image mask M being projected to a lower dimension. We have denoted this information preservation parameter as inf and used it as a tuning parameter for our defense mechanism.

3. Defense Mechanism

As illustrated in Figure 2, the proposed ODDR defense technique encompasses three stages. The initial stage involves splitting the image into kernels using a moving window. This fragmentation process deconstructs the image into equally sized chunks, the dimensions of which are fine-tuned as hyper-parameters for specific applications. This stage is referred to as Fragmentation. Subsequently, the obtained fragments are flattened into vectors, and the outlier detection task is executed on these vectors, denoted as Feature Segregation. Finally, Dimension Reduction is applied to a window positioned on the cluster of fragments identified as outliers. This step aims to neutralize the adversarial patch without compromising information in the surrounding vicinity. The entire algorithm is detailed in 1, with each component and function elucidated in the subsequent subsections.

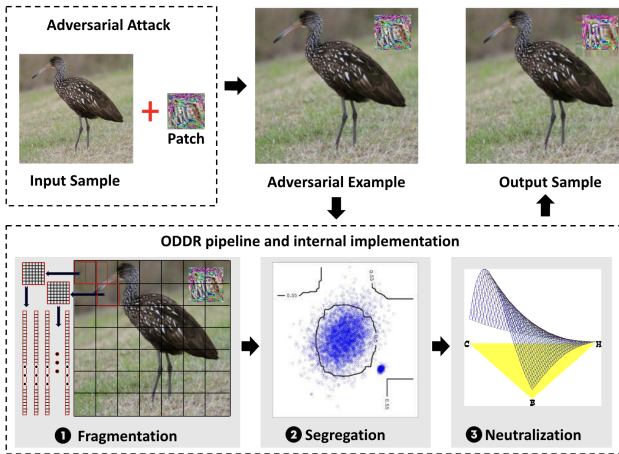


Figure 2. Overview of the Proposed ODDR Defense Methodology: The three-stage pipeline—Fragmentation, Segregation, and Neutralization—demonstrating the process of identifying and mitigating adversarial patches in the input image features.

Algorithm 1: ODDR: Outlier Detection & Dimension Reduction

IN : I : original image, k : kernel size, str : stride length, c : confidence of anomalies, T : number of trees in isolation forest, d : size of square mask, inf : information preserved after SVD
OUT : I' : Image with neutralised patch
*/*Fragmentation*/*
 Generate n fragments $X \leftarrow (x_1, \dots, x_n)$ from image I , using kernel size = k and stride = str
*/*Segregation*/*
 Set $s = 0.3 \times \text{Size}(X)$
 $iForest = \text{IsolationForest}(X, T, s)$ (Algo 2)
 initialize $Y = (y_1, \dots, y_n)$
 for $i = 1$ to n do:
 $y_i = \text{Score}(x_i)$, where $x_i \in X$ (From Eq. 2)
 end for
 Sort Y in descending order
 Select $(1 - c) * n$ top y_i s as anomalies
 $(z_1, \dots, z_r) \rightarrow Z$
*/*Neutralization*/*
 Select biggest cluster in Z
 Calculate cluster center z_{cen} , $z_{cen} \in Z$
 Create Mask M of size d , from $z_{cen} - (d/2)$ to $z_{cen} + (d/2)$
 $M' \leftarrow \text{SVD}(M, inf)$
 Superimpose M' in place of M in image I to get I'
 return I'

3.1. Fragmentation

The initial step in processing the input image is Fragmentation. This involves segmenting the image into partially overlapping fragments using a moving square kernel. The size of this kernel, along with the stride length determining the movement for each new fragment, is a system hyper-parameter fine-tuned for optimal performance. Upon generating the fragments, each with three channels and a square shape, the data is flattened into long vectors. This flattening is a crucial preparatory step for the subsequent stage in the process, Feature Segregation.

3.2. Segregation

The notion of segregation of anomalous input features within the feature space is carried out as an outlier detection exercise. We propose that an ensemble of isolation trees, which is an isolation forest, is best suited for this purpose. The fragments generated using the aforementioned Fragmentation process serves as the dataset for the outlier detection algorithm. The anomaly detection using Isolation Forests is outlined in Algorithm 2, which

Algorithm 2: *IsolationForest*($X, T, size$)

IN: $X = (x_1, \dots, x_n)$: input data, T : number of trees in the forest, s : sample size
OUT: an *IsolationForest* (*IsolationTrees* ensemble)
initialize : *IsolationForest*
set $l_{max} = \text{ceiling}(\log_2 S)$
for $i = 1$ to T **do:**
 $X' \leftarrow \text{Sample}(X, s)$
 IsolationForest \leftarrow *IsolationForest* \cup
 IsolationTree($X', 0, l_{max}$)
end for
return *IsolationForest*

is essentially an ensemble of Isolation Trees which are generated using Algorithm 3. Once the trees are generated, the path lengths for the leaf nodes are calculated using the Equation 1, which is thereafter used to estimate the anomaly score using the Equation 2, as described in Section 2. Once the anomaly scores are ascertained to each fragment, the top outliers are selected based on a pre-defined threshold, which is set as a hyper-parameter. Among the detected outliers, the largest co-located cluster is chosen, and its cluster center is identified. Notably, the overlapping nature of the fragments, by design, implies that once the a cluster of anomalous fragments is selected, the center of the fragment is considered as the center in general. A window of a stipulated size, also a hyper-parameter to the system, is marked around the cluster centre and that window is used as a mask. This mask is thereafter subjected to dimension reduction. Importantly, for Object Detection tasks, determining the size of the mask in advance can be challenging. Therefore, it is set dynamically during the algorithm’s execution, often matching the size of the cluster of anomalies or the number of outlier fragments.

3.3. Neutralization

The mask derived from the Segregation process encompasses the entirety or, at the very least, the majority of the adversarial patch, whether naturalistic or otherwise. This assertion is grounded in the fact that the mask is chosen from the region where the cluster of anomalies or outlier fragments is situated. Comprehensive testing and validation of this approach are presented in the Experiments section (4) later in the paper.

To render the detected adversarial patch ineffective, two techniques have been explored. The first approach, though sub-optimal, involves replacing each pixel in the mask with the mean value of all the pixels within the region covered by the mask. This method performs effectively when the mask aligns closely with the adversarial patch. However, for a broader region, it may result in a potential loss of valuable

Algorithm 3: *IsolationTree*(X, h, l_{max})

IN: $X = (x_1, \dots, x_n)$: input data, h : height of tree, l_{max} : maximum height of tree, Q : attributes of X
OUT: an *IsolationTree*
if $h \geq 1$ or $|X| \leq 1$, **then:**
 return *externalNode*{ $Size \leftarrow |X|$ }
else
 $X_{left} \leftarrow \text{Select}(X, q < p)$, where
 $\min(q) \leq p < \max(q)$, $q \in Q$
 $X_{right} \leftarrow \text{Select}(X, q \geq p)$, where
 $\min(q) \leq p < \max(q)$, $q \in Q$
 return *internalNode*
 {
 LeftTree \leftarrow
 IsolationTree($X_{left}, h + 1, l_{max}$)
 RightTree \leftarrow
 IsolationTree($X_{right}, h + 1, l_{max}$)
 attribute $\leftarrow q$
 value $\leftarrow p$
 }
end if

information in areas where the mask does not overlap with the adversarial patch. To solve this problem, we propose Dimension Reduction. We apply a singular value decomposition on the mask, with a specific hyper-parameter that selects the proportion of information to preserve (corresponding to the number of singular values). The details of this is explained in Section 2. Either way, both of these techniques are computationally much simpler than the use of neural network based in-painting that is used in many defense techniques available in the literature [24].

4. Experimental Results

In this section, we thoroughly assess the effectiveness of our proposed defense mechanism.

4.1. Experimental Setup

We assess ODDR performance across diverse settings commonly employed in computer vision applications:

Task: Classification -

Datasets: We employ the ImageNet dataset [7] for its extensive class variety and the Caltech-101 dataset [19] for specific object recognition tasks.

Models: Our assessment encompasses ResNet-152 [15], ResNet-50 [15], and VGG-19 [22] for ImageNet and Caltech-101 classification tasks.

Task: Detection -

Datasets: For outdoor detection challenges, we use the INRIA dataset [6], capturing uncontrolled environmental

variations. For indoor scenarios, we utilize the CASIA datasets [27].

Models: The YOLO model [1] is employed for detection tasks. we test both outdoor and indoor scenarios.

Threat Model: We operate under the assumption of a white-box scenario, where the attacker possesses complete knowledge of the victim DNN, including its architecture and parameters. As in other proposed defenses [17, 21, 26], the adversary is capable of substituting a specific region of an image with an adversarial patch, with the goal of consistently inducing targeted misclassification across all input instances.

Patch-based Attacks: In this evaluation, we use four state-of-the-art adversarial patches, illustrated in Figure 3. Specifically, the Adversarial Patch [9] and LAVAN [8] are applied to assess classification tasks, while the AdvYOLO adversarial patch [25] and the Naturalistic Patch [16] are chosen for the evaluation of detection tasks. These patches represent cutting-edge techniques in the domain, ensuring a robust and comprehensive assessment of the ODDR defense mechanism across different challenges.



Figure 3. Illustration of different adversarial patches used in our defense evaluation.

4.2. Results

Throughout the experiments, we used a kernel size of 20x20 pixels, with a stride length of 10 for Fragmentation. For Segregation we varied the confidence of anomalies c between 0.8–0.85 and used 500 trees in the isolation forest. For the Dimension Reduction using SVD, the information preservation parameter is varied between 70 – 85%.

4.2.1 ODDR in Classification Benchmarks

In our evaluation, the primary focus was on measuring the model’s robust accuracy. To illustrate the impact of our defense strategy, we initially generated adversarial patches using two distinct attack strategies, namely LAVAN and GoogleAp. Subsequently, we reported the model’s robust accuracy across different patch sizes and various models. The performances of ODDR on clean samples without the patches are 79.8% (ResNet-152), 77.3% (ResNet-50) and 73.2% (VGG-19) on ImageNet and 92.8% (ResNet-152), 88.9% (ResNet-50) and 87.1% (VGG-19) on CalTech-101.

Multiple patch sizes were considered, with the complete set of results being reported in the supplementary materials.

Tables 1 and 2 highlight the impressive performance of our defense technique, showcasing a remarkable level of robust accuracy when countering GoogleAp and LAVAN attacks on the ImageNet dataset. For instance, our defense achieves robust accuracy rates of 79.1% and 74.1% when employed against GoogleAp and LAVAN attacks, respectively.

Patch Size	Model / Neural Network	Baseline Accuracy	Adversarial Accuracy	Robustness (w/ patch)
38	ResNet 152	81.2%	39.9%	79.1%
x	ResNet 50	78.4%	38.8%	75.6%
38	VGG 19	74.2%	39.1%	72.8%

Table 1. ODDR robustness on GoogleAp attack (ImageNet dataset)

Patch Size	Model / Neural Network	Baseline Accuracy	Adversarial Accuracy	Robustness (w/ patch)
38	ResNet 152	81.2%	10.1%	74.1%
x	ResNet 50	78.4%	10.2%	70.2%
38	VGG 19	74.2%	11.1%	71.1%

Table 2. ODDR robustness on LAVAN attack (ImageNet dataset)

Similarly, on the Caltech-101 dataset, ODDR achieves outstanding performance with robust accuracy rates of 90.8% and 91.1% when defending against GoogleAp and LAVAN attacks, respectively.

Patch Size	Model / Neural Network	Baseline Accuracy	Adversarial Accuracy	Robustness (w/ patch)
38	ResNet 152	94.1%	48.6%	90.8%
x	ResNet 50	90.9%	49.2%	86.4%
38	VGG 19	88.6%	47.1%	85.6%

Table 3. ODDR robustness on GoogleAp attack (CalTech-101 dataset)

Patch Size	Model / Neural Network	Baseline Accuracy	Adversarial Accuracy	Robustness (w/ patch)
38	ResNet 152	94.1%	15.6%	91.1%
x	ResNet 50	90.9%	17.1%	87.3%
38	VGG 19	88.6%	15.3%	84.9%

Table 4. ODDR robustness on LAVAN attack (CalTech-101 dataset)

4.2.2 ODDR in Detection Benchmarks

In the context of detection tasks, we report Robust Average Precision and Recovery Rate in Table 5 against AdvYOLO

Dataset	Clean Avg. Precision	Adversarial Avg. Precision	Robust Avg. Precision
INRIA	96.42%	39.28%	83.21%
CASIA	96.77%	32.25%	93.54%

Table 5. Performance of our proposed defense ODDR in terms of average precision against AdvYOLO [25] attack for INRIA and CASIA datasets.

Defense	Adversarial Accuracy	Robust Accuracy
LGS [21]	39.26%	53.86%
Jujutsu [5]	39.26%	60%
Jedi [24]	39.26%	64.34%
DS[17]	39.26%	35.02%
PG [26]	39.26%	30.96%
Ours	39.9%	79.1%

Table 6. Performance of our proposed defense compared to five state-of-the-art empirical defenses and two certified in Classification benchmark (GoogleAp [9] attack).

[25] attack for INRIA and CASIA datasets. The Recovery Rate quantifies the proportion of outputs recovered by the defense in relation to the total number of successful attacks. It accurately reflects the inherent positive impact of the defense mechanism. Our defense technique achieves a high robust average precision of 93.54% and 83.21% for INRIA and CASIA datasets respectively.

4.3. ODDR vs State-of-the-art

We conduct a comparative analysis of ODDR against LGS [21], Jujutsu [5] and Jedi [24] across all previously outlined experiments. Additionally, for illustrative purposes, we compare ODDR with two certified defenses—namely, De-randomized smoothing [17], and PatchGuard [26]. As depicted in Table 6, our defense technique surpasses state-of-the-art techniques. Specifically, our approach achieves a robust accuracy of 79.1%, outperforming LGS, Jujutsu, and Jedi defenses, which achieve 53.86%, 60%, and 64.34% robust accuracy, respectively.

We also compare our defense with two certified defenses, although the comparison is unfair, we aim to quantify the cost associated with ensuring provable robust defense on overall performance. As anticipated, the performance of certified adversarial patch defenses was lower than that of empirical defenses, as illustrated in Table 6. These results underscore the trade-off between provable robustness and empirical utility, highlighting the limitations in the practical effectiveness of certified adversarial patch defenses.

In detection tasks, as demonstrated in Tables 7 and 8, our defense outperforms in terms of both robust average

Defense	Robust Avg. Precision	Recovery Rate
LGS [21]	21%	27%
Jedi [24]	28.03%	42%
Ours	82.14%	43.86%

Table 7. Performance of our proposed defense ODDR compared to two state-of-the-art defenses against AdvYOLO [25] attack for INRIA dataset.

Defense	Robust Avg. Precision	Recovery Rate
LGS [21]	84%	48%
Jedi [24]	80%	50%
Ours	93.54%	61.29%

Table 8. Performance of our proposed defense ODDR compared to two state-of-the-art defenses against AdvYOLO [25] attack for CASIA dataset.

precision and recovery rate when deployed against the advYOLO patch, across both INRIA and CASIA datasets.

4.4. Key Findings

The key findings from our extensive experimentation across different machine learning tasks and corresponding benchmarks are noted below:

- For Image Classification tasks, the proposed ODDR performs exceptionally well as is able to reach robust performance within 1 – 3% range of the clean baseline accuracies across different models, datasets and adversarial patches, as shown in Tables 1, 2, 3, 4. As reported, this technique has a very low false positive rate, with the drop in accuracy of the clean samples subjected to ODDR is within a 1 – 2% range.
- For Object Detection tasks, ODDR performs equally well, and is consistently able to reach robust performance within 3 – 5% of clean baseline accuracies, with a highly impressive performance recovery for the CASIA dataset shown in Table 5.
- For both Image Classification and Object Detection tasks, our proposed ODDR significantly outperforms the defense techniques available in the literature. Specifically, for Classification, ODDR outperforms both empirical defenses and certified defenses (shown in Table 6) by at least 15% as compared to the best of the lot. For Object Detection, ODDR outperforms the other defense techniques across datasets as shown in Tables 7 and 8.
- The proposed ODDR technique is able to thwart naturalistic patches equally as well, which have been created to better blend in the scene to prevent detection, matching and even outperforming the state-of-the-art, as evident from Tables 9 and 10 respectively.

Defense	Robust Avg. Precision	Recovery Rate
LGS [21]	55%	29%
Jedi [24]	63%	51%
Ours	65%	47%

Table 9. Performance of our proposed defense compared to five state-of-the-art defenses against Naturalistic Patch [16] attack for INRIA dataset.

Defense	Robust Avg. Precision	Recovery Rate
LGS [21]	50%	48%
Jedi [24]	67%	76%
Ours	87.5%	90.27%

Table 10. Performance of our proposed defense compared to five state-of-the-art defenses against Naturalistic Patch [16] attack for CASIA dataset.

5. Discussion

The proposed ODDR technique identifies the adversarial noise in the patches as an outlier to the data distribution of the rest of the input sample. It is worth noting here that upon detection, there is no requirement of substituting the patch with generative fill and a simple dimension reduction technique (essentially simple matrix transformation) is sufficient to render the patch ineffective at a much smaller computational cost. To further test the limit of robustness of ODDR, we also used naturalistic patches [16] and have successfully mitigated such attacks.

5.1. ODDR vs. Naturalistic Patches

A recent adversarial patch generation method that poses a potentially greater challenge to our defense is the Naturalistic Patch [16]. We investigate the effectiveness of this attack strategy, considering its ability to generate stealthy adversarial patches that mimic real objects, rendering them less visually suspicious and, consequently, more challenging to detect. The results, specifically the recovery rate upon using ODDR, are presented in Tables 9 and 10. Despite the naturalistic nature of this patch and its seamless integration into the image, our defense successfully mitigated its adversarial impact.

5.2. Impact of ODDR on Model Interpretability

We conduct a detailed visualization of the Grad-CAM [23] output for the adversarial example, both before and after the application of our defense mechanism. Notably, as shown in Figure 4, we observe a significant shift in the network’s focus when the adversarial patch is applied, as the attention shifts from the actual object to the manipulated patch. However, upon applying our defense, we observe a

restoration of the network’s attention back to the original object, highlighting the efficacy of our defense in preserving the model interpretability.

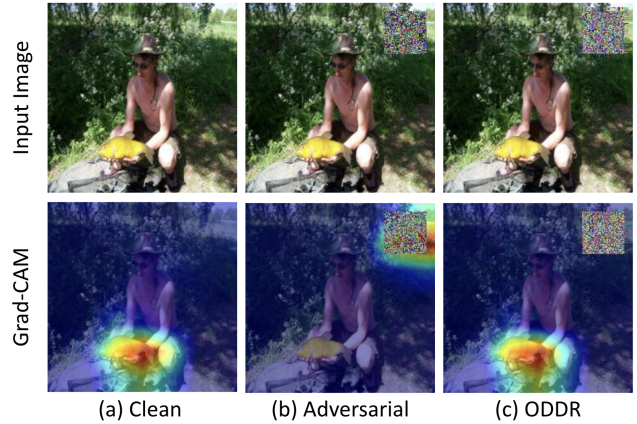


Figure 4. Grad-CAM visualization result for ODDR in action

6. Related Works

There are two approaches to defense against such attacks: empirical defenses and certified defenses.

Empirical defenses: **Localized Gradient Smoothing (LGS)** [21] first normalizes gradient values and then uses a moving window to identify high-density regions based on certain thresholds. **Jujutsu** [5] focuses on localizing adversarial patches and distinguishing them from benign samples, and uses generative adversarial networks to reconstruct the “clean” examples from adversarial examples. **Jedi** [24] is based on an input entropy analysis and recovering the image using inpaint. These defenses, while valuable, do come with certain limitations such as high false positive rates, poor detection rates,

Certified defenses: **De-randomized smoothing (DS)** [17] introduces a certified defense technique by building a smoothed classifier by ensembling local predictions made on pixel patches. **PatchGuard (PG)**[26] uses enforcing a small receptive field within deep neural networks (DNNs) and secure feature aggregation.

7. Conclusion

We propose ODDR (Outlier Detection and Dimension Reduction), specifically designed to counteract the formidable threat posed by patch-based adversarial attacks on machine learning models. This technique leverages a three-stage pipeline—Fragmentation, Segregation, and Neutralization — which effectively identifies and mitigates adversarial patches while preserving crucial information for machine learning tasks. Through rigorous experimentation on benchmark datasets and state-of-the-art adversarial

patches, we substantiate its effectiveness on robustness on multiple machine learning tasks, whilst demonstrating minimal loss in clean accuracies.

Acknowledgment

This research was partially funded by Technology Innovation Institute (TII) under the "CASTLE: Cross-Layer Security for Machine Learning Systems IoT" project.

References

- [1] Alexey Bochkovskiy, Chien-Yao Wang, and Hong-Yuan Mark Liao. Yolov4: Optimal speed and accuracy of object detection. *arXiv preprint arXiv:2004.10934*, 2020. **6**
- [2] N. Carlini and D. A. Wagner. Towards evaluating the robustness of neural networks. *CoRR*, abs/1608.04644, 2016. **1**
- [3] Nandish Chattopadhyay, Anupam Chattopadhyay, Sourav Sen Gupta, and Michael Kasper. Curse of dimensionality in adversarial examples. In *2019 International Joint Conference on Neural Networks (IJCNN)*, pages 1–8. IEEE, 2019. **3**
- [4] Nandish Chattopadhyay, Subhrojyoti Chatterjee, and Anupam Chattopadhyay. Robustness against adversarial attacks using dimensionality. In *International Conference on Security, Privacy, and Applied Cryptography Engineering*, pages 226–241. Springer, 2021. **3**
- [5] Zitao Chen, Pritam Dash, and Karthik Pattabiraman. Jujutsu: A two-stage defense against adversarial patch attacks on deep neural networks. In *Proceedings of the 2023 ACM Asia Conference on Computer and Communications Security*, page 689–703, New York, NY, USA, 2023. Association for Computing Machinery. **1, 7, 8**
- [6] N. Dalal and B. Triggs. Histograms of oriented gradients for human detection. In *2005 IEEE Computer Society Conference on Computer Vision and Pattern Recognition (CVPR'05)*, pages 886–893 vol. 1, 2005. **2, 5**
- [7] Jia Deng, Wei Dong, Richard Socher, Li-Jia Li, Kai Li, and Li Fei-Fei. Imagenet: A large-scale hierarchical image database. In *2009 IEEE Conference on Computer Vision and Pattern Recognition*, pages 248–255, 2009. **2, 5**
- [8] Dan Karmon et al. Lavan: Localized and visible adversarial noise. In *International Conference on Machine Learning*, 2018. **6**
- [9] Tom Brown et al. Adversarial patch. 2017. **2, 6, 7**
- [10] D Freedman, R Pisani, and R Purves. Statistics. 2007. ISBN: 0-393970-833, 1978. **3**
- [11] I. J. Goodfellow, J. Shlens, and C. Szegedy. Explaining and harnessing adversarial examples. *CoRR*, abs/1412.6572, 2015. **1**
- [12] Amira Guesmi, Ruitian Ding, Muhammad Abdullah Hanif, Ihsen Alouani, and Muhammad Shafique. Dap: A dynamic adversarial patch for evading person detectors, 2023. **1**
- [13] Amira Guesmi, Muhammad Abdullah Hanif, Bassem Ouni, and Muhammad Shafique. Physical adversarial attacks for camera-based smart systems: Current trends, categorization, applications, research challenges, and future outlook. *IEEE Access*, 11:109617–109668, 2023. **1**
- [14] Sahand Hariri, Matias Carrasco Kind, and Robert J Brunner. Extended isolation forest. *IEEE transactions on knowledge and data engineering*, 33(4):1479–1489, 2019. **3**
- [15] Kaiming He, Xiangyu Zhang, Shaoqing Ren, and Jian Sun. Deep residual learning for image recognition. In *Proceedings of the IEEE conference on computer vision and pattern recognition*, pages 770–778, 2016. **5**
- [16] Yu-Chih-Tuan Hu, Jun-Cheng Chen, Bo-Han Kung, Kai-Lung Hua, and Daniel Stanley Tan. Naturalistic physical adversarial patch for object detectors. In *2021 IEEE/CVF International Conference on Computer Vision (ICCV)*, pages 7828–7837, 2021. **1, 2, 6, 8**
- [17] Alexander Levine and Soheil Feizi. (de) randomized smoothing for certifiable defense against patch attacks. *Advances in Neural Information Processing Systems*, 33: 6465–6475, 2020. **1, 6, 7, 8**
- [18] B. Li and Y. Vorobeychik. Scalable optimization of randomized operational decisions in adversarial classification settings. In *Proceedings of the Eighteenth International Conference on Artificial Intelligence and Statistics, AISTATS 2015, San Diego, California, USA, May 9-12, 2015*. JMLR.org, 2015. **1**
- [19] Fei-Fei Li, Marco Andreoto, Marc’Aurelio Ranzato, and Pietro Perona. Caltech 101, 2022. **5**
- [20] Fei Tony Liu, Kai Ming Ting, and Zhi-Hua Zhou. Isolation forest. In *2008 eighth IEEE international conference on data mining*, pages 413–422. IEEE, 2008. **3**
- [21] Muzammal Naseer, Salman Khan, and Fatih Porikli. Local gradients smoothing: Defense against localized adversarial attacks. In *2019 IEEE Winter Conference on Applications of Computer Vision (WACV)*, pages 1300–1307. IEEE, 2019. **1, 6, 7, 8**
- [22] Karen Simonyan and Andrew Zisserman. Very deep convolutional networks for large-scale image recognition. *arXiv preprint arXiv:1409.1556*, 2014. **5**
- [23] Akshayvarun Subramanya, Vipin Pillai, and Hamed Pirsiavash. Towards hiding adversarial examples from network interpretation. *CoRR*, abs/1812.02843, 2018. **8**
- [24] Bilel Tarchoun, Anouar Ben Khalifa, Mohamed Ali Mahjoub, Nael Abu-Ghazaleh, and Ihsen Alouani. Jedi: Entropy-based localization and removal of adversarial patches. In *Proceedings of the IEEE/CVF Conference on Computer Vision and Pattern Recognition*, pages 4087–4095, 2023. **1, 5, 7, 8**
- [25] Simen Thys, Wiebe Van Ranst, and Toon Goedemé. Fooling automated surveillance cameras: adversarial patches to attack person detection. *CoRR*, abs/1904.08653, 2019. **2, 6, 7**
- [26] Chong Xiang, Arjun Nitin Bhagoji, Vikash Sehwal, and Prateek Mittal. {PatchGuard}: A provably robust defense against adversarial patches via small receptive fields and masking. In *30th USENIX Security Symposium (USENIX Security 21)*, pages 2237–2254, 2021. **1, 6, 7, 8**
- [27] Shiqi Yu, Daoliang Tan, and Tieniu Tan. A framework for evaluating the effect of view angle, clothing and

carrying condition on gait recognition. In *18th international conference on pattern recognition (ICPR'06)*, pages 441–444. IEEE, 2006. [2](#), [6](#)